FRACTURE SAFETY OF LIQUEFIED NATURAL GAS TANK IN CRYOGENIC CONDITIONS

G An, Department of Naval Architecture and Ocean Engineering, Chosun University, Republic of Korea, **J Park,** Department of Civil Engineering, Chosun University, Republic of Korea, **D Seong,** Department of Naval Architecture and Ocean Engineering, Chosun University, Republic of Korea, **I Han,** Technical Research Laboratory, POSCO, Republic of Korea

SUMMARY

High-manganese austenitic steel has been developed as a new cryogenic steel for application in liquified natural gas (LNG) storage and fuel tanks, with improved fracture toughness and safety at cryogenic temperatures. Generally, the fracture toughness decreases at lower temperatures; therefore, cryogenic steel requires a high fracture toughness to prevent unstable fractures. This study conducted unstable ductile fracture tests with 30-mm-thick high-manganese austenitic steel and evaluated its applicability to LNG storage and fuel tanks. The ductile fracture resistance in the weld joints was evaluated, including the weld metal and heat-affected zone. The unstable fracture resistance was evaluated for different LNG tank types. It was found that high-manganese austenitic steel has excellent unstable fracture characteristics and good material performance as a cryogenic steel; therefore, it can be applied in LNG storage and fuel tanks.

KEYWORDS

unstable ductile fracture; fracture toughness; cryogenic steel; LNG storage/fuel tank; crack tip opening displacement test; wide plate tensile test

NOMENCLATURE

ν	Poisson's ratio
σ_y	Offset yield stress
P	Pressure (N m-2)
LNG	Liquified natural gas
IMO	International Maritime Organization
STS	Stainless steel
CTOD	Crack tip opening displacement
FCC	Face-centered cubic
HAZ	Heat-affected zone
SAW	Submerged arc welding
WM	Weld metal
FL	Fusion line
IGC	International Code for the Construction and Equipment of Ships Carrying Liquefied Gases in Bulk
ISO	International Organization for Standardization
WES	Welding Engineering Society

1. INTRODUCTION

Liquefied natural gas (LNG) is used as a raw material for city gas and as a fuel for power generation worldwide; however, owing to global environmental problems such as the safety of nuclear power and global warming caused by carbon dioxide in recent years, its features as a clean energy source are being significantly re-evaluated. Recently, serious environmental problems caused by carbon have emerged, and countries worldwide have been declaring carbon neutrality (Lanqing, 2022). In this context, the application of eco-friendly fuels has become essential for transportation. Container ships for economical transportation have become larger of late (i.e., above 22,000 TEU (Twenty-foot Equivalent Unit)); hence, there has been an increase in the demand for stronger and thicker steel plates in the shipbuilding industry. Accordingly, Yield Point (YP) 460 MPa class or higher-grade steel with a thickness of 80–100 mm has been introduced in the construction of real ship structures (Inoue, 2006, Kawabata, 2010, Handa, 2010, Inoue, 210). As such, even ultra-large vessels are recently being built using an engine-propelled method that can use eco-friendly fuel. Recently, an ultra-large container ship using LNG as a propulsion fuel has been built and is currently sailing.

In the case of ships, low-quality fossil fuels are used. Correspondingly, the International Maritime Organization (IMO) 2020 regulation significantly strengthened the upper limit of sulfur content in marine fuel oil from 3.5% to 0.5% to reduce or prevent emissions of sulfur oxides from January 1, 2020, forward (IMO, 2019). Therefore, newly built ships have begun to be constructed based on eco-friendly fuels such as LNG, ammonia, and hydrogen. LNG is not a fully eco-friendly fuel, as it contains carbon. However, in reality, the application of hydrogen and ammonia as completely eco-friendly fuels remains technically difficult. Therefore, LNG is currently used as a semi-environmental fuel for

transportation. LNG is stored at a cryogenic temperature of -165 °C to reduce its volume. Therefore, LNG should be stored in special vessels constructed using cryogenic steels such as 9% Ni steel, stainless steel (STS) 304, and aluminium alloys (Machida, 1993, Niu. 2020); however, these materials have disadvantages, e.g., high fluctuations in steel prices and difficult welding (Niu. 2020). In addition, it is important to secure the various properties of the base material and welded joints in cryogenic (-163 °C or below) environments to ensure fracture safety for improved applicability (Kang, 2004).

In the past, conventional cryogenic steels such as 9% Ni steel and aluminium alloy (A5083-0) have been used in LNG storage tanks (IGC code, 2020, IGF code, 2020). When increasing the size of the storage tank, it is necessary not only to study the strength design, but also to thoroughly study the characteristics of the materials used, their workability and weldability, and other construction methods, as well as to provide quality control. In particular, it is necessary to estimate the characteristics of the base metal and weld joint fracture safety at cryogenic temperatures, including the risk of brittle fracture. Only the steels listed in the IMO International Code for the Construction and Equipment of Ships Carrying Liquefied Gases in Bulk (IGC)/International Code of Safety for Ship Using Gases or Other Low-flashpoint Fuels code can be utilized for cryogenic steel, and only 9%Ni steel, STS, and aluminium alloy are listed in the code(IGC code, 2020, IGF code, 2020). In addition, a recently developed high-manganese austenitic steel interim guideline was adopted by the IMO(2018); hence, high-manganese austenitic steel can be utilized as a cryogenic steel.

In general, cryogenic steels should have excellent impact toughness at cryogenic temperatures and excellent resistance to brittle fracture. There is also risk of unstable ductile fracture (Machida, 1991, 1993, Watanabe, 1984). Among the cryogenic steels utilized in the past, 9% Ni steel has a martensitic microstructure, and there is a risk of brittle fracture (Machida, 1991, 1993). Regarding high-manganese austenitic steel and STS 304, there is little risk of brittle fracture owing to the austenitic structure; however, the possibility of an unstable ductile fracture exists (Machida, 1991, 1993, An, 2017). Therefore, to utilize cryogenic steel in LNG storage and fuel tanks, it is necessary to investigate the safety and/or risk of unstable destruction in cryogenic environments. In general, fracture toughness decreases with decreasing service temperature, and fracture toughness has become an important mechanical property when investigating material fracture and failure mechanics (Masubuchi, 1980, Anderson, 2005, Ripling, 1982, Andrea, 2006, Vantadori, 2013, Carpinteri, 2015).

In this study, the unstable fracture characteristics of welded joints with high-manganese austenitic steel were studied by applying it to large LNG storage tanks in shipbuilding. In particular, the allowable crack length was

derived from the design load by evaluating the fracture resistance performance according to crack propagation to secure an unstable fracture. In addition, the crack tip opening displacement (CTOD) wide plate tensile test, a representative fracture toughness evaluation, was performed to evaluate the safety of unstable fractures potentially occurring at cryogenic temperatures. Based on the experimental results, the safety of high-manganese austenitic steel, a novel cryogenic steel, was evaluated in a cryogenic environment.

2. MATERIALS AND TEST METHODS

2.1 SPECIMEN PREPARATION

High-manganese austenitic steel (such as STS 304) has a face-centred-cubic (FCC) structure, and the matrix structure is composed of austenite. In general, the austenite structure has excellent cryogenic fracture stability and does not undergo brittle fracture, even at cryogenic temperatures. The material utilized in the experimental examination was high-manganese austenitic steel with over 22% Mn and an FCC crystal structure. Tables 1 and 2 list the chemical compositions and mechanical properties of the high-manganese austenitic steel, respectively. High-manganese austenitic steel with a thickness of 30 mm (the upper limit for the construction of LNG storage and fuel tanks) was utilized for the test steel plate. Most steels used for cryogenic applications comprise predominantly FCC crystal structures to ensure the good low-temperature toughness required for cryogenic structures. High-manganese austenitic steel has an FCC crystal structure for cryogenic LNG tank applications. The yield strength was 444 MPa, the tensile strength was 822 MPa, and the impact toughness was 105 J at -196 °C; these characteristics satisfy the IGC code standard values (IGC code, 2020, IGF code, 2020).

Table 1: Chemical composition of the base metal

(wt. %)

C	Si	Mn	P	S
0.35–0.55	0.10–0.50	22.5–25.50	Max. 0.03	Max. 0.01

Table 2: Mechanical properties of base metal using the plate-bar type tensile specimen

Yield stress (MPa)	Tensile strength (MPa)	Elongation (%)	Charpy impact energy, at-196 °C (J)
444	822	56	105 (transverse direction)

2.2 EXPERIMENTAL WELDING METHOD

Welding specimens were prepared to investigate the unstable fracture characteristics of the weld metal (WM) and heat-affected zone (HAZ). The submerged arc welding

(SAW) process used to manufacture LNG tanks was applied to manufacture the test specimens. In general, SAW is applied as in the context of a horizontal welding part when manufacturing LNG tanks. Table 3 lists the experimental welding procedure for the SAW process. The heat input of each welding pass was 3.0 kJ/mm. In addition, a welding consumable with a strength lower than that of the base material was used. The tensile strength of the base material was 822 MPa, i.e., very high, whereas that of the WM was 667–780 MPa, i.e., considerably lower. Therefore, the test specimen utilized in this study was applied to under-matched joints. A schematic of the sample preparation process for a 30-mm-thick steel plate weld of cryogenic steel is illustrated in Figure 1. The groove shape was a single 40° V-groove with a 6-mm root gap and a straight weld line was created for evaluating the fracture toughness in the HAZ.

Table 3: Submerged arc welding (SAW) conditions

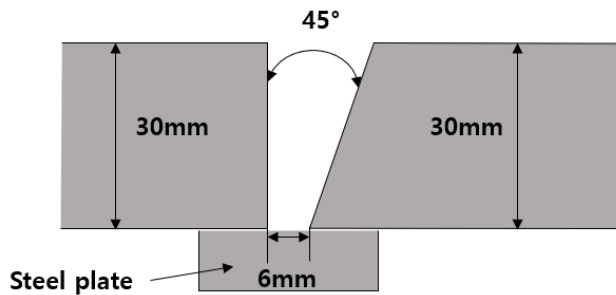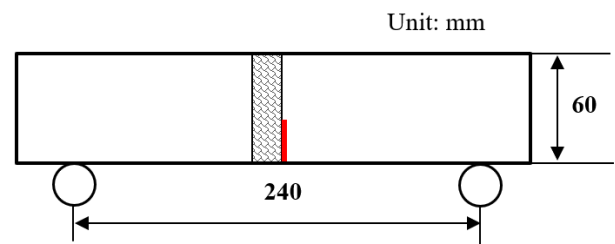| Thick. (mm)	Current (A)	Voltage (V)	Speed (cm/min)	Heat input (kJ/mm)
30	580	28	32	3.0

Figure 1. Schematic of the sample preparation process for 30-mm-thick steel plate weld
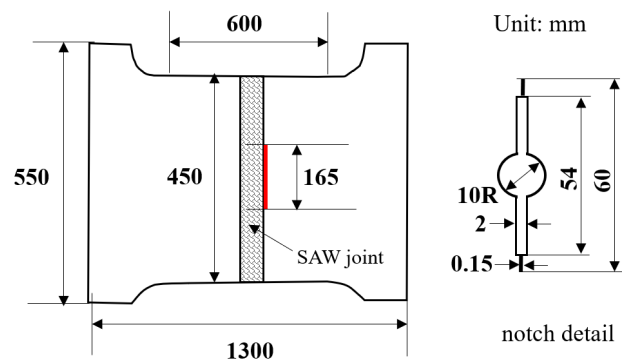
2.3   UNSTABLE FRACTURE TEST METHOD

The CTOD test is a typical fracture-toughness evaluation method. In this study, CTOD specimens were prepared to evaluate the fracture safety at cryogenic temperatures. In addition, wide-plate test specimens were prepared to evaluate the fracture toughness in real structures. The test specimen shapes are shown in Figure 2. Regarding the brittle fracture characteristics, the toughness was determined by a three-point bending CTOD test for the base metal, WM, and HAZ (Figure 2 (a)). A full-thickness notch penetration wide plate test was performed on the WM and HAZ to evaluate the ductile fracture characteristics (Figure 2 (b)). Generally, an austenitic microstructure material fracture mode becomes a ductile fracture at cryogenic temperatures (Machida, 1993), and the high-manganese austenitic steel utilized in this study had an austenitic structure; therefore, a ductile failure was expected. The welding consumables had microstructures similar to that of the base material. Conventionally, 9% Ni steel has a martensitic structure and is prone to brittle

fractures at cryogenic temperatures. It exhibits excellent fracture toughness at cryogenic temperatures; therefore, it is possible to arrest brittle cracks even if brittle fracture occurs (Machida, 1993). High-manganese austenitic steel has a low possibility of brittle fracture (An, 2021), but the possibility of an unstable ductile fracture exists. Therefore, a three-point bending CTOD test and wide tensile test with a central notch were performed to evaluate the unstable ductile fracture phenomenon. The test specimen shapes are shown in Figure 2. In addition, to confirm the fracture safety, wide plate tensile test (WPT) was performed with a cross-weld joint with a thickness penetration notch.

(a) Crack tip opening displacement (CTOD) specimen geometry of weld joint

(b) Wide-plate test specimen geometry of weld joint

Figure 2. Test specimens for evaluating unstable ductile fracture of high-manganese austenitic steel

3.   TEST RESULTS AND DISCUSSION

To apply high-manganese austenitic steel in onshore and offshore LNG storage tanks, its safety in cryogenic environments should be verified. For the occurrence of ductile cracks, the characteristics were evaluated using a commonly CTOD experiment. In addition, a CTOD R-curve was used to examine the ductile fracture resistances of the three-point bending CTOD specimens and a wide plate tensile specimen. As this material is to be utilized in cryogenic environments, it was necessary to investigate the safety of unstable fractures.

3.1   BRITTLE CRACK INITIATION BEHAVIOR

The results from the brittle fracture toughness test (CTOD) at −165 °C using the base metal, WM, fusion

line (FL), and FL+2 mm (FL+2) based on International Organization for Standardization (ISO) 12135 and 15653 (DNV, 2013, Newman, 1981, JWES, 2011, ASTM, 1997) are shown in Figure 3. The P-V curves of all specimens show the type(6) mode, indicating that a brittle fracture did not occur in all notch positions. This is a typical characteristic of austenitic microstructure steel, and all of the specimens exhibit extremely excellent brittle fracture resistance. The high-manganese austenitic steel has a similar microstructure to stainless steel, which has a stable growth of ductile cracks without brittle fracture even at cryogenic temperatures. As illustrated in the P–V curve of the CTOD experiment, a brittle fracture does not occur even at cryogenic temperatures, and the ductile cracks grow stably.

3.2 INITIAL CRACK AND CRACK PROPAGATION CHARACTERISTICS IN WELD JOINTS

High-manganese austenitic steel is known to have excellent arrestability during brittle crack propagation, and thus there is little possibility of brittle fracture in the welds (An, 2021). The applicability of high-manganese austenitic steel in the manufacture of LNG storage tanks was evaluated based on the fracture mechanics. High-manganese austenitic steel has a sufficient brittle crack prevention ability to prevent brittle fracture. In the unlikely event that a brittle crack occurs owing to an unforeseen event, it is necessary to have the ability to prevent brittle crack propagation before it leads to a large-scale fracture accompanied by a liquid outflow. However, as the strength of the base metal of high-manganese austenitic steel is higher than that of the WM, when cracks exist in the weld FL, the brittle crack does not propagate along the HAZ. Instead, it diverts to the WM, which has low strength, and becomes a ductile fracture. Therefore, the WM must be able to prevent unstable ductile crack propagation.

In general, to evaluate the fracture safety of LNG tanks, it is assumed that T-welded joints are commonly generated during the manufacture of welded structures such as LNG tanks. As shown in Figure 4, in this study, we considered the defect at a cross part along the horizontal weld joint. Generally, flux-cored arc welding and SAW are used for construct of LNG tanks. In this study, the fracture safety was evaluated for the case of an unstable ductile fracture occurring in the weld joints by an external load after fatigue crack propagation (assuming that the cracks occur in the horizontal welds). To evaluate unsafe fractures, it is important to assume an initial crack size. A more conservative crack size was determined by comparing the results of a previous study (Machida, 1993) with the crack size determined by classification rules (DNV,

2013). In previous research, the crack length and depth were set to 1.5 to 0.2 times the thickness as the initial crack, respectively (Machida, 1993). However, in the Det Norske Veritas classification rules for butt joints (DNV, 2013), the crack size in the HAZ part is defined as 1.0 mm in depth and 5 mm in length. In this study, to more conservatively set the initial crack size, 1.5 times the thickness was set as the initial crack size. Thus, a crack length of 45 mm and depth of 6 mm were set as the initial defect sizes. Figure 5 shows a schematic diagram of the assumed initial crack length and fatigue crack propagation process.

In addition, the crack length when the brittle fracture occurred and arrested after the fatigue cracks progressed by a certain size from the initial defect was assumed to be 5.5 times the thickness in the previous study. However, in the case of the high-manganese austenitic steel used in this study, as brittle fracture does not occur, the conditions that can actually occur were evaluated. In LNG tanks, a cyclic fluctuating stress occurs owing to fluctuations in the liquid level owing to the loading and unloading of the contents, and it is necessary to investigate the propagation of fatigue cracks from the initial defects owing to this stress change. As for the stress condition, it is assumed that the content is subjected to repeated empty and full conditions for a severe evaluation, and the crack propagates from the first cycle while maintaining a semi-elliptical shape. In the case of the LNG tank, assuming that liquid is received approximately 40 times a year and the service life is 25 years, the total number of cycles is 1,000 (Machida, 1993). The stress intensity factor (K) of a semi-elliptical surface crack was calculated based on the Newman equations (Newman, 1981). The fatigue crack propagation is evaluated as follows, as proposed by the Japan Welding Engineering Society (WES) 2805 (JWES, 2011).

$$\frac{da}{dN} = C\left(\Delta K^m - \Delta K_{th}\right) \tag{1}$$

In the above, $C = 2.60 \times 10^{-11}$, $m = 2.75$, and $\Delta K_{th} = 2.00\left(MPa\sqrt{m}\right)$.

Based on the final crack size considering the fatigue crack growth, a method based on WES-2805 was applied to calculate the fracture toughness value required to prevent the initiation of the brittle fracture from the defect. Table 4 presents the results. Despite the extremely conservative evaluation, the propagation of fatigue cracks owing to cyclic stress did not occur. It can be seen that the critical CTOD value required for the weld zone FL is approximately 0.09 mm. As shown in Figure 3, the minimum CTOD value of the high-manganese austenitic steel weld joints is 0.48 mm or more at -165 °C. Thus, it can be said that there was no risk of brittle fracture.
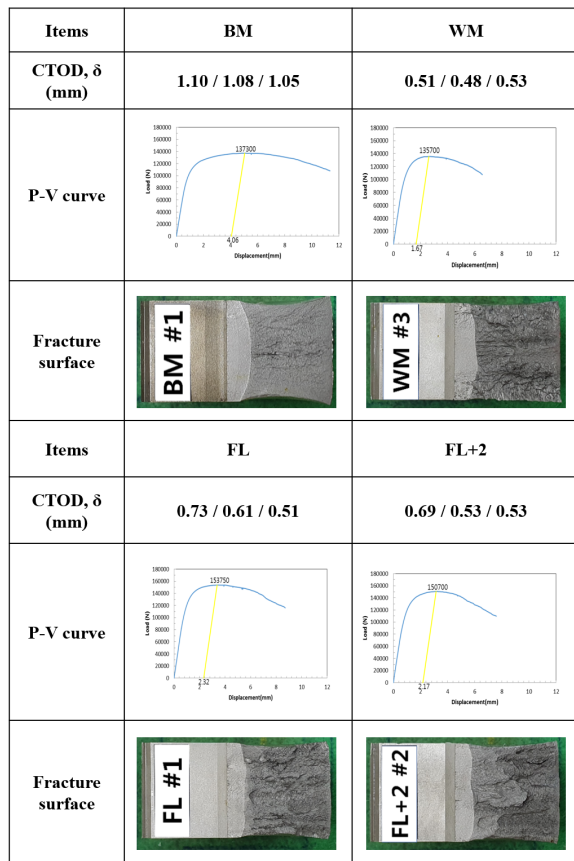
Items	BM	WM
CTOD, δ (mm)	1.10 / 1.08 / 1.05	0.51 / 0.48 / 0.53
P-V curve		
Fracture surface		
Items	FL	FL+2
CTOD, δ (mm)	0.73 / 0.61 / 0.51	0.69 / 0.53 / 0.53
P-V curve		
Fracture surface		

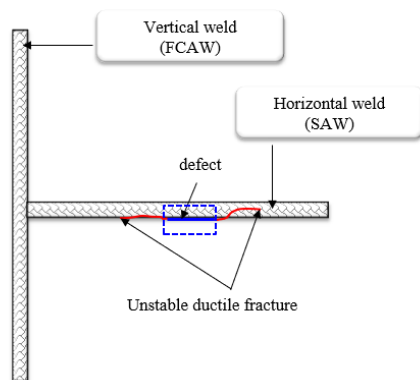Figure 3. CTOD test results at -165 °C with base metal and weld joints

Figure 4. Defect location and weld line of liquified natural gas (LNG) storage tank
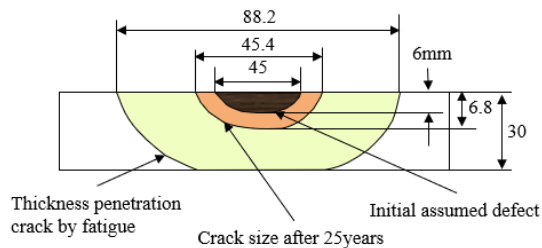

Figure 5. Schematic diagram of fatigue crack propagation

Table 4: Estimation of fatigue crack propagation after 25 years and required crack tip opening displacement (CTOD) at design stress.

Initial crack size (mm)		Final crack size after 25 years (mm)		Required CTOD (mm) (σ=189MPa)
2c	a	2c	a	
45	6	45.4	6.8	0.094

Where, 2c and a are initial crack length and depth.

Even when the LNG tank was used for 25 years, the propagation of cracks owing to fatigue from the initial defects was insignificant. In the case of high-manganese austenitic steel, there is little risk of brittle fracture; therefore, the possibility of brittle crack propagation was not considered in this study. The crack length was calculated considering the case where the initial crack penetrated the thickness of the specimen owing to fatigue instead of the growth of the initial crack owing to brittle crack propagation and arrest. Table 5 presents the results from the fatigue crack propagation calculations. The initial defect length of 45 mm and depth of 6 mm advanced until the depth of the crack reached 30 mm in the thickness direction and the crack length advanced to 88.2 mm. However, as a result, the crack length was shorter than 165 mm, i.e., 5.5 times the thickness proposed in a previous study (Machida, 1993). Therefore, for the most conservative evaluation in this study, the final defect size of the specimen for the evaluation of unstable fracture safety was set to 165 mm.
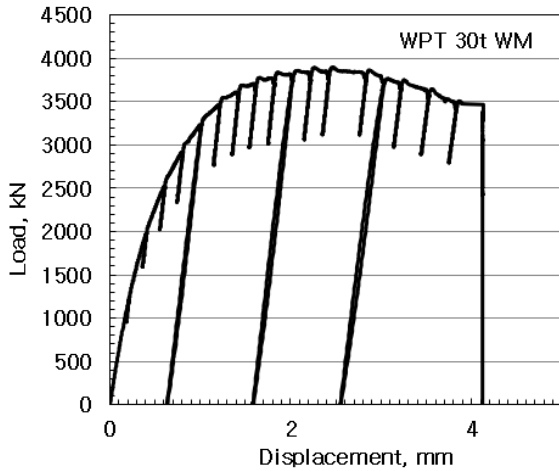
Table 5: Estimation of fatigue crack propagation after thickness penetration

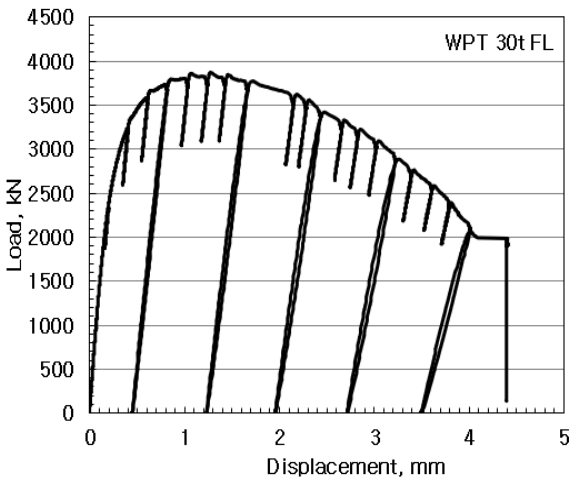| Initial defect (crack) size		Final defect size (Max. 189 MPa)	
2c	a	2c	a
45mm	6mm	88.2mm	30.0mm

3.3 CHARACTERISTICS TO PREVENT UNSTABLE DUCTILE FRACTURE

High-manganese austenitic steel exhibits a negligible possibility of brittle fracture at cryogenic temperatures; therefore, it was mainly necessary to evaluate the possibility of unstable ductile fracture (An, 2021). Wide-plate tensile tests and three-point bending CTOD tests were performed on the weld joints to evaluate the unstable ductile fracture resistance of the high-manganese austenitic steel. Figure 6 shows the load-displacement relationship of the wide-plate tensile test. The wide-plate tensile test was performed
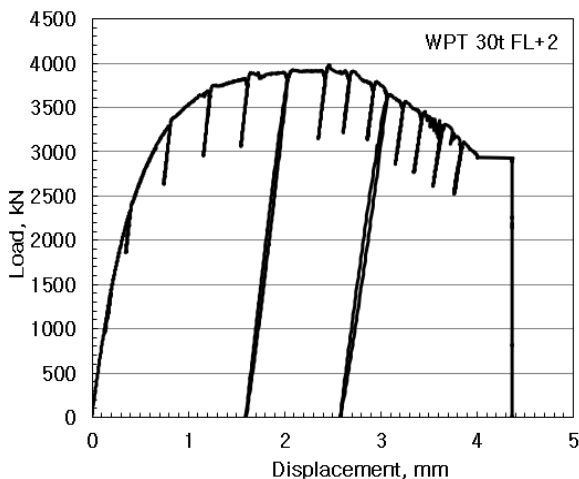
at room temperature with three types of notch position specimens, i.e., WM, FL, and FL+2 notch specimens. In the tests, the unloading compliance method (Garwood, 1979, Kifner, 1973) was used to measure the ductile crack length. The wide-plate tensile test was conducted using a 10,000 kN universal testing machine in the tensile loading mode, as shown in Figure 6 (d).

(a) weld metal

(b) fusion line

(c) fusion line+2mm

(d) WPT experiment photo

Figure 6. Example of wide plate test R-curve recorded at room temperature.
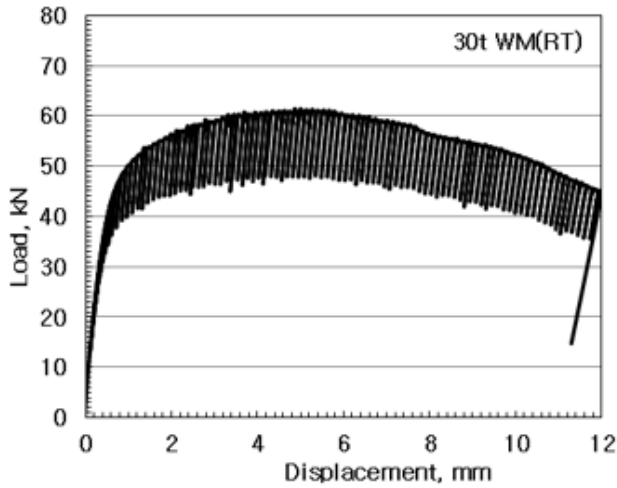
The same tests were carried out with bend type specimens to evaluate of fracture toughness compare with tensile type specimens. The bend type specimen shows more conservative result compare with tensile type specimen test results. Figure 7 shows the relationship between the ductile crack length and resistance value obtained at room temperature and at −165 °C for the WM and FL+2 specimens using the three-point bending CTOD test. The CTOD test specimen had a wider width of 4 B (B: specimen plate thickness) to investigate the ductile crack length over a wide area. The load increased at cryogenic temperature rather than at room temperature and the displacement decreased; however, the value was insignificant. Owing to the characteristics of high-manganese austenitic steel, there is almost no possibility of brittle fracture, even at cryogenic temperatures. Therefore, it was experimentally confirmed that brittle fracture has never occurred as the crack progressed; nevertheless, continuous displacement occurred.

The crack extension length was determined from experimental displacement data using Equation (2), according to ASTM E813-89 (ASTM, 1979). This equation corresponds to the unloading compliance method with both the tensile-WPT and bending-CTOD loading modes.
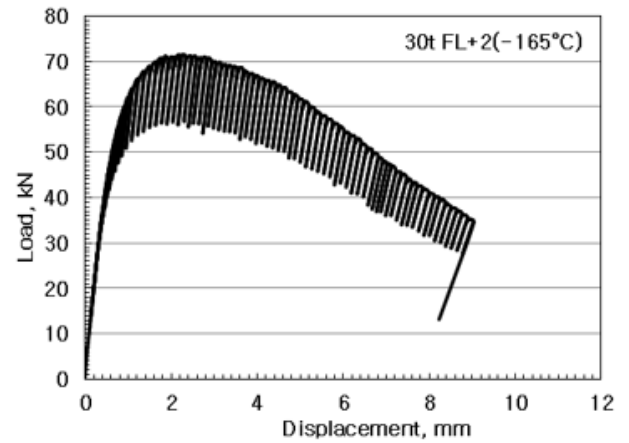
$$\frac{a_n}{W} = 0.999748 - 3.9504U_x + 2.9821U_x^2$$

$$- 3.21408U_x^3 + 51.5156U_x^4 - 113.031U_x^5 \qquad (2)$$

$$U_x = 1 / \left[\left(\frac{4BWEV}{PS} \right)^{\frac{1}{2}} \right]$$

Here, W, B, and S are the geometric shapes of the specimen, E is the Young's modulus, V is the clip gauge displacement, and P is the load.
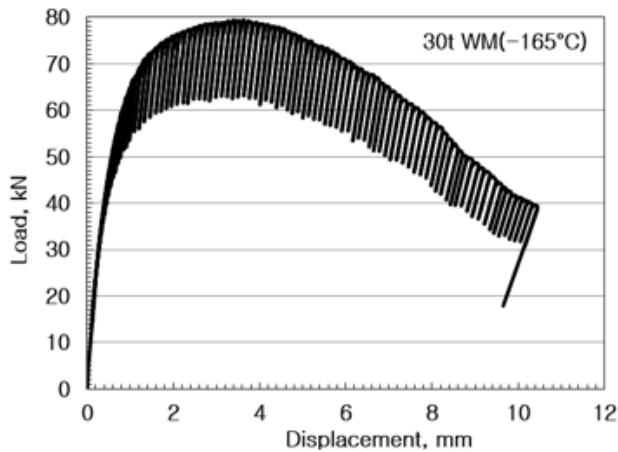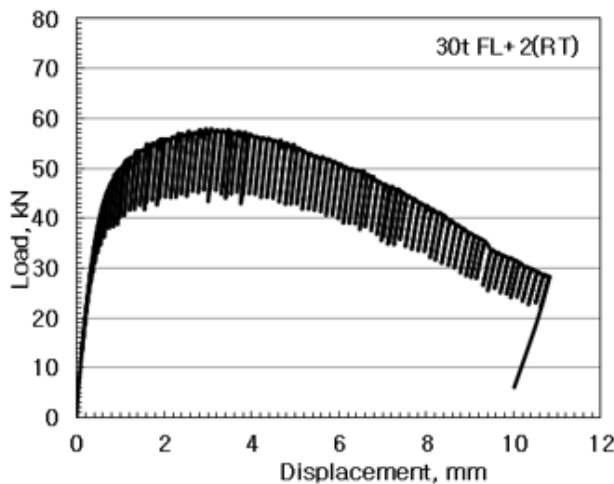
(a) weld metal at R.T.

(d) fusion line +2mm at -165°C

Figure 7. Example of bending test R-curve recorded at room temperature and -165 °C

(b) weld metal at -165°C

The calculation of the δ_R value was based on the Wells equation given by Equation (3) for comparison with conventional results (Tanaka, 1988). As the δ_R value is extremely large, it can be considered that the result is approximately similar to that from ISO 15653, which is usually performed.
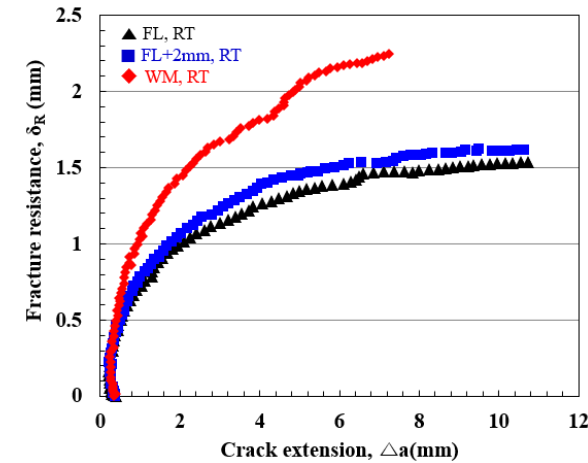
$$\delta_R = \left[\frac{0.45(W-a_n)}{(0.45W+0.55a_n+Z)}\right] \times \left[V - \frac{\gamma \sigma_y W(1-\upsilon^2)}{E}\right] \quad (3)$$

In the above, σ_y is 0.2% of the offset yield stress, and ν is Poisson's ratio.
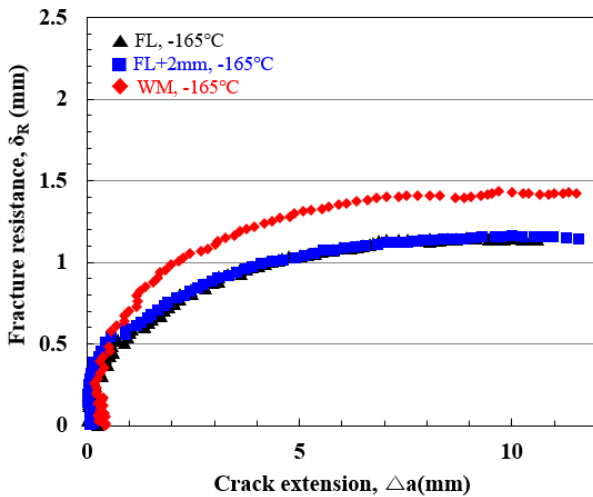
$$\gamma = 3.3956X + 1.9282X^2 - 7.10161X^3 + 4.0484X^4,$$
$$(X = a_n / W)$$

Figure 8 shows the fracture resistance and δ_R curve (relationship between fracture resistance and crack extension) as obtained in the three-point bending CTOD tests with the WM, FL, and FL + 2 specimens at (A) room temperature and (b) -165 °C. It is known that the crack propagation resistance performance is lower in a bending loading mode than in a tensile loading mode (Garwood, 1979). Therefore, in this study, the crack propagation tests were conducted at cryogenic temperatures under the more conservative bending loading mode, and the crack propagation resistance curves were evaluated. Based on previous research results, the effect of the test method on the δ_R value was evaluated between the wide-plate and three-point bending tests. The wide-plate test indicated a 1.5 times larger value of δ_R at a similar test temperature (An, 2021). The δ_R curve with respect to the ductile crack length increases steeply at first, but then becomes gentle. When it progresses to approximately 8 mm, it becomes almost horizontal, and the resistance value reaches its maximum in all specimens, i.e., the δ_R-plateau (Tanaka, 1988). The δ_R-plateau values of the WM, FL, and FL+2 specimens under each condition are 2.35 mm, 1.52 mm, and 1.61 mm at room temperature, respectively, and 1.42 mm, 1.15 mm, and 1.14 mm at -165 °C, respectively. The ductile

(c) fusion line +2mm at R.T.

fracture resistance at room temperature is excellent, and the FL and FL+2 specimens show a similar performance. The ductile crack resistance performance of the WM is the best in this research experiment. In the case of the WM, the strength is lower than that of the base material and it has excellent fracture resistance; this is considered to result in slightly superior performance. At cryogenic temperatures, the ductile fracture resistance performance decreases compared to that at room temperature; however, in the FL and FL+2 specimens, the level is maintained at approximately 70% of that at room temperature.

(a) δ_R curves at R.T.

(b) δ_R curves at -165°C

Figure 8. Fracture resistance curves with weld metal (WM), fusion line (FL), and FL+2mm

The safety of high-manganese austenitic steel when applied to LNG tanks can be examined by evaluating its fracture mechanics. Using the CTOD-R curve obtained from the experiment, an unstable ductile fracture was investigated for the crack assumed in the WM, FL, and HAZ FL+2 parts of the LNG tank. With respect to the circumferential
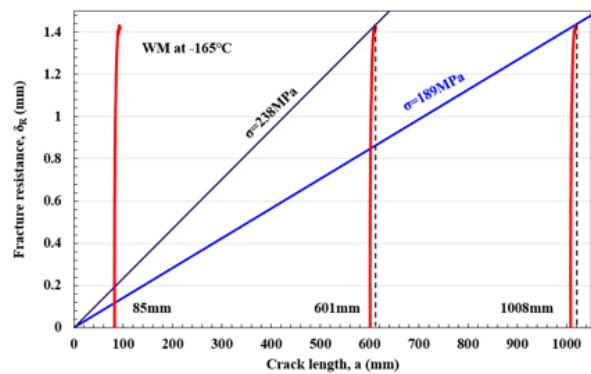
stress in the joint crack, the crack bulges from the inside when the content flows out (bulenting), thereby increasing the driving force of the crack. The CTOD considering this bulenting effect was obtained by correcting the Dugdale crack model (Kifner, 1973).

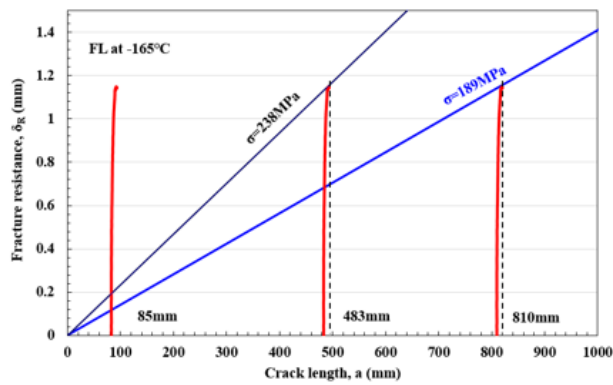$$\delta = 8\sigma_y a / \pi E \cdot \ln\left[\sec(\pi M \sigma / 2\sigma_y)\right] \qquad (4)$$

Here, M : folias factor $= \left[1 + 2.51X - 0.054X^2\right]^{1/2}$, and $X = a^2 / Dt$. D is the LNG tank size, and t is the thickness.

Figure 9 shows the relationship between the fracture resistance and crack length for each allowable stress using Equation (4), where the allowable stresses for the B-type- and C-type LNG tanks are 189 MPa and 264 MPa, respectively. The allowable stress of the LNG tank was calculated using the formula for austenitic steel defined in IMO IGC codes [6]. In addition, for a conservative evaluation of fracture safety, the R curve obtained in the three-point bending test was adopted. An unstable ductile fracture occurs at the point where the R curve (δ_R) moves parallel to the crack length and tangents the driving force line (δ) of the crack (Machida, 1984). Figure 9 shows the maximum allowable crack length at which an unstable ductile failure does not occur at each allowable stress for the WM, FL, and FL+2 mm specimens. For the allowable stress of the C-type LNG tank (189 MPa), even if the crack length is 800 mm or greater, it does not lead to an unstable ductile fracture. In addition, with respect to the allowable stress of the B-type LNG tank (238 MPa), an unstable ductile failure does not occur, even when the crack propagates up to 80 mm. Therefore, there is no possibility of an unstable ductile fracture owing to the cracks generated in high-manganese austenitic steel weld joints.
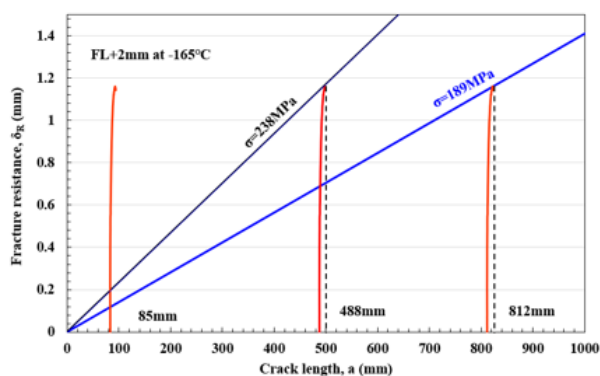
In addition, when there is an initial crack of 2a = 5.5t (=165 mm), the stress for unstable ductile fracture is 436 MPa, i.e., providing a very large margin with respect to the allowable stress. From the results, it can be concluded that there is no risk of unstable ductile fracture in high-manganese austenitic steel weld joints.

(a) weld metal at -165°C

(b) fusion line at -165℃

(c) fusion line +2mm at -165℃

Figure 9. Ductile fracture instability analysis for crack in SAW with WM, FL, and FL+2 mm

4. CONCLUSIONS

In this study, the unstable fracture characteristics of a high-manganese austenitic steel plate used in an applicable LNG storage tank were investigated. In particular, the unstable ductile fracture toughness in weld joints, which determines the risk of unstable fracture, was investigated using a large-scale wide-plate test and three-point bending test under cryogenic conditions. The results are as follows.

(1) The high-manganese austenitic steel weld joints have excellent material properties; therefore, the WM and HAZ did not exhibit brittle manner after the maximum load, and showed ductile fracture even in a cryogenic environment. No brittle fracture occurred even after the maximum load was reached, and the fracture surface exhibited only the ductile fracture at cryogenic temperatures.

(2) At cryogenic temperatures, the unstable ductile fracture resistance was reduced compared to that at room temperature, and the performance of the WM was superior to that of the HAZ.

(3) The unstable ductile fracture resistance performance values under the allowable stress for each LNG storage tank type at cryogenic temperatures were evaluated. The allowable crack lengths of the WM and HAZ under the largest allowable stress conditions were 600 mm and 480 mm, respectively.

In this study on high-manganese austenitic steel applied to an LNG storage tank, a safety evaluation was conducted for the case where a crack that starts from a weld defect, advances owing to fatigue, and causes an unstable ductile failure. Based on these results, it was determined that high-manganese austenitic steel has excellent unstable fracture characteristics and good material performance as a cryogenic steel; therefore, it can be applied in LNG storage and fuel tanks.

5. ACKNOWLEDGEMENTS

6. REFERENCES

1. LANQING, LI., XIUHENG, WANG., JINGYU, MIAO., ALIYA, ABULIMITI., XINSHENG, JING. AND NANQI, REN. (2022). *Carbon neutrality of wastewater treatment - A systematic concept beyond the plant boundary.* Environmental Science and Ecotechnology. 11: 1-7.

2. INOUE, T., ISHIKAWA, T., IMAI, S., KOSEKI, T., HIROTA, K. AND TADA., M. (2006). *Long crack arrestability of heavy-thick shipbuilding steels.* Proceeding of the 16th International Offshore and Polar Engineering Conference. 4: 132-136.

3. KAWABATA, T., MATSUMOTO, K., ANDO, T., YAJIMA, H., AIHARA, S. AND YOSHINARI, H. (2010). *Development of brittle crack arrest toughness Kca test method – brittle crack arrest design for large container carrier ships – 2.* Proceeding of the 20th International Offshore and Polar Engineering Conference. 4: 80–87.

4. HANDA, T., MATSUMOTO, T., YAJIMA, H., AIHARA, S., YOSHINARI, H. AND HIROTA, K. (2010). *Effect of structural discontinuities of welded joints on brittle crack propagation behavior–brittle crack arrest design for large container carrier ships–3.* Proceeding of the 20th International Offshore and Polar Engineering Conference. 4: 88–94.

5. INOUE, T., YAMAGUCHI, Y., YAJIMA, H., AIHARA, S., YOSHINARI, H, AND HIROTA, K. (2010). *Required brittle crack arrest toughness Kca value with actual scale model tests–brittle crack arrest design for large container carrier ships– 4.* Proceeding of the 20th International Offshore and Polar Engineering Conference. 4: 95–101.

6. INTERNATIONAL MARITIME ORGANIZATION. (2019). *IMO 2020* - cleaner shipping for cleaner air.

7. MACHIDA, S., DEGUCHI, A. AND KAGAWA, H. (1993). *Brittle fracture characteristics of heavy gauge 9% Ni steel plate for large scale LNG storage tank.* Journal of High Pressure Institute of Japan. 31: 31-38.

8. NIU, W., LIN J., JU, Y. AND FU, Y. (2020). *The daily evaporation rate test and conversion method for a new independent type B LNG mock-up tank.* Cryogenics. 111: 1-11.

9. KANG, S., KIM, M., KIM, Y., SHIN, Y. AND LEE, H. (2004). *A Study on the Fracture Toughness Characteristics of FCAW Weldment of Steel for Offshore Structures.* Journal of Korea Welding and Joining Society. 22 (6): 57-63.

10. IGC CODE. (2020). *Code for the Construction and Equipment of Ships Carrying Liquefied Gases in Bulk.* International Maritime Organization.

11. IGF CODE. (2020). *International code of safety for ships using gases or other low-flashpoint fuels.* International Maritime Organization.

12. INTERNATIONAL MARITIME ORGANIZATION. (2018). *Interim guidelines on the application of high manganese austenitic steel for cryogenic service.*

13. MACHIDA, S., ISHIKURA, N., KUBO, N., KATAYAMA, N., MURAMOTO, S., HAGIWARA, Y. AND ARIMOCHI, K. (1993). *Fracture Characteristics of Heavy Thickness 9% Ni Steel Plate and its Applicability to Large Scale LNG Storage Tanks (2nd Report, High Toughness 50-55mm Thick 9% Ni Steel Plate).* Journal of High Pressure Institute of Japan. 31: 19-33.

14. MACHIDA, S., ISHIKURA, N., KUBO, N., KATAYAMA, N., MURAMOTO, S., HAGIWARA, Y. AND ARIMOCHI, K. (1991). *Brittle fracture characteristics of heavy thickness 9% Ni steel plate and its applicability to large scale LNG storage tanks.* Journal of High Pressure Institute of Japan. 29: 25-39.

15. WATANABE, I., SUZUKI, M., MATSUDA, Y., YAMAGATA, S. AND YAJIMA, H. (1984). *The crack-arrest properties of 9% Ni steel and its weldment (1st report).* Bulletin of the Japan Society of Naval Arch and Ocean Engineering. 155: 389-400.

16. WATANABE, I., SUZUKI, M., MATSUDA, Y., YAMAGATA, S., AND YAJIMA. H. (1984). *The crack-arrest properties of 9% Ni steel and its weldment (2nd report).* Bulletin of the Japan Society of Naval Arch and Ocean Engineering. 155: 401-407.

17. AN, G., HONG, S., PARK, J., RO, C., AND HAN. I. (2017). *Identification of Correlation Between Fracture Toughness Parameters of Cryogenic Steel Weld Joints.* Journal of Welding and Joining. 35: 82-87.

18. MASUBUCHI, K. (1980). *Analysis of Welded Structures-Fracture toughness. 1st edition.* Pergamon. New York: 336-399.

19. ANDERSON, T. (2005). *Fracture mechanics. 3rd edition.* CRC Press.

20. RIPLING, J. AND CROSLEY, B. *Crack arrest fracture toughness of a structural steel(A36).* (1982). Welding Research.: 65-74.

21. ANDREA, C., ROBERTO, B. AND SABRINA, V. (2006). *Notched shells with surface cracks under complex loading.* International Journal of Mechanical Sciences. 48: 638-649.

22. VANTADORI, S., CARPINTERI, A., AND SCORZA, D. (2013). *Simplified analysis of fracture behaviour of a Francis hydraulic turbine runner blade.* Fatigue and Fracture of Engineering Materials and Structures. 36 (7): 679-688.

23. CARPINTERI, A., RONCHEI, C., SCORZA, D., AND VANTADORI, S. (2015). *Fracture mechanics based approach to fatigue analysis of welded joints.* Engineering Failure Analysis. 49: 67-78.

24. MACHIDA, S., ISHIKURA, N., KUBO, N., KATAYAMA, N., MURAMOTO, S., HAGIWARA, Y. AND ARIMOCHI, K. (1993). *Fracture Characteristics of Heavy Thickness 9% Ni Steel Plate and its Applicability to Large Scale LNG Storage Tanks.* The Japan Society of High Pressure Science and Technology. 31: 19-33.

25. AN, G., PARK, J., PARK, AND HAN, I. (2021). *Fracture Toughness Characteristics of High-Manganese Austenitic Steel Plate for Application in a Liquefied Natural Gas Carrier.* metals. : 1-13.

26. DET NORSKE VERITAS AS. (2013). *DNV Rules for Ships.* Det Norske Veritas.

27. NEWMAN, J. AND RAJU, I. (1981). *An Empirical Stress Intensity Factor Equation For Surface Crack.* Engineering Fracture Mechanics, 15(1-2): 185-192

28. THE JAPAN WELDING ENGINEERING SOCIETY, (2011). *Method of assessments for flaws in fusion welded joints with respect to brittle fracture and fatigue crack growth.* The Japan Welding Engineering Society.

29. AMERICAN SOCIETY FOR TESTING AND MATERIALS E813-89. (1997). *Test Method for JIC, A Measure of Fracture Toughness.* American Society for Testing and Materials.

30. TANAKA, K. (1988). *Regarding safety evaluation of materials for large cryogenic storage tanks research.* University of Tokyo dissertation.

31. GARWOOD, J. (1979). *Effect of specimens germetry on crack growth resistance.* Fracture Mechanics. Am. Soc. Test. Mater. 677: 511–532.

32. KIFNER, J., MAXEY, W., EIBER, R. AND RFFY, A. (1973). *Failure Stress Levels of Flaws in Pressurized Cylindes.* ASTM STP 356: 461

33. MACHIDA, S. (1984). *Ductile fracture mechanics, Nikkan Kogyo Shimbun.*: 43-53.